Scientific Research

Martensitic Characterization of the $Ti_{45.3}Ni_{54.7}$ Melt Spun Alloy

Geroge C. S. Anselmo, Walman Benicio de Castro[*], Carlos J. de Araújo

UAEM, Universidade Federal de Campina Grande, Aprígio Veloso, Brazil.
Email: georgeanselmo@yahoo.com.br, [*]walman@dem.ufcg.edu.br, carlos@dem.ufcg.edu.br

ABSTRACT

The ribbons of the $Ti_{45.3}Ni_{54.7}$ shape memory alloy were prepared through the melt spinning technique. The study was focused on investigating the effect of the rapid solidification and grain size at characteristic start martensitic (M_s), final martensitic (M_f), start austenite (A_s) and final austenite (A_f) transformation temperatures. Changes on martensitic transformation temperatures in $Ti_{45}Ni_{55}$ melt spun ribbons were observed as grain size is reduced. Results of optical microscopy and differential scanning calorimetry (DSC) were used to associate grain size with transformation temperatures.

1. Introduction

Shape memory alloys (SMAs) represent a unique class of materials that undergo a reversible phase transformation (martensitic transformation) allowing these materials to display dramatic pseudoelastic stress-induced deformations and recoverable temperature-induced shape memory deformations. These materials are used as smart materials in a variety of aerospace, biomechanical, and microelectronics applications. Among the known shape memory alloys, Ni-Ti is the most commonly used because of its excellent mechanical properties, corrosion resistance and biocompatibility [1]. In the recent past, the field of microsystems has been subject to growing attention from both the industry and the research community. Microsystems have been recognized as having the potential to revolutionize the performance of a wide range of products by merging silicon-based microelectronics with micromachining technologies, thus enabling complete systems-on-a-chip to be developed and allowing novel functionalities at reduced costs. In this context, the application of shape memory alloys for actuation of micropneumatic devices might bring a relevant technological breakthrough. SMA materials exhibit the highest energy density amongst current micro-electromechanical systems MEMS compatible materials and, more importantly, as size is reduced towards the micro-scale, they benefit from improved heat transport, which increases their response speed [2].

Many studies have been undertaken to find a method to control the martensitic transformation. According to previous studies, it is significantly affected by the alloy composition, crystallographic defects such as dislocations, precipitation and grain size [3]. Grain boundaries are believed to strengthen parent phases, and therefore Ms decreases with decreasing grain size. In Ti-Ni-based alloys, the critical austenite grain size for martensitic transformation is known to be 50 nm, below which martensitic transformation does not occur.

The aim of this work is to study the relationship between grain size and martensitic transformation temperature in the $Ti_{45.3}Ni_{54.7}$ alloy. In order to attain a wide range of cooling rate and grain size, the melt spinning technique is therefore considered a suitable preparation route for this alloy. Melting spinning is an important method for producing metals with improved mechanical and/or physical properties. This technique employs a very high cooling rate (up to $10^{6\circ}C/s$). In general, such a high cooling rate has the advantage of refinement of grain sizes [4].

2. Experimental Procedure

The $Ti_{45.3}Ni_{54.7}$ ingot with 19 mm in diameter by 100 mm long was prepared using the conventional vacuum arc-remelting (VAR) method. High purity Ti and Ni raw materials were repeatedly melted six times in an argon atmosphere for homogenization. Then they were cut into

small pieces, each of which has a weight in the range of 10 to 30 grams, induction-melted in an argon atmosphere in a quartz crucible at 1250°C supplied into a single-roller melt-spinning machine and subsequently ejected by high pressurized argon out of a 0.4 mm orifice onto a 200 mm diameter copper roller with at different tangential speeds between 30 and 50 m/s. The final ribbons of the melt-spinning process ranged between 30 μm and 41 μm in thickness and 1 mm in width. Transformation temperatures and enthalpies of as-spun ribbons were determined by differential scanning calorimetry TA Q20 DSC with 10 °C/min heating and cooling rate and the temperature scanning range was from −30 to +200°C. The software for DSC for data acquisition, storage and evaluation under MS WINDOWS. It has multitasking with simultaneous operation of several thermal analysis systems and simultaneous evaluation graphical user surface, integrated detailed HELP system. Microstructure of cross-section of ribbons was examined by Nikon FX-35DX optical microscope (OM). For optical microscopy, the specimens were polished using conventional procedures and etched in a solution composed of HF: HNO_3: H_2O = 4: 5: 10 (in volume). The etching time was about 10 - 15 s. From the OM images under 1000× magnification, the average grain size of ribbons was estimated by the linear intercept method [5]. The numbers of intercepted grains were at least 10 and 50 for large and small grains, respectively.

3. Results and Discussion

The wheel velocity was changed from 30 to 50 m/s while the melt spinning temperature was fixed at 1350°C. **Figure 1** shows the thickness of as-spun $Ti_{45}Ni_{55}$ alloy ribbons as a function of the melt spinning wheel velocity.

The increase of the wheel velocity from 30 to 50 m/s results in a decrease of the ribbon thickness from 41 μm to 30 μm. As the increase of the wheel velocity leads to a
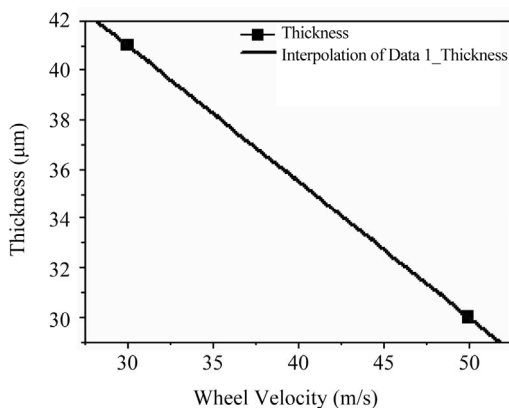
reduced ribbon thickness, the heat transfer coefficient at the quenching wheel-ribbon interface is enhanced and the cooling rate increases. Therefore, this result clearly indicates that variations in the melt spinning temperature and wheel velocity allow the effective control of the cooling rates in the melt spinning process.

Figure 2 shows optical micrographs of as-spun ribbons fabricated at two different wheel velocities of 30 and 50 m/s. As seen in **Figure 2**, as-spun $Ti_{45.3}Ni_{54.7}$ ribbons are fully crystallized and most of the columnar and small grains are located at the free surface and copper roller surface of the ribbons, respectively.

Refined grain structure is the hypothesis to the decrease in the transformation temperature, as shown in **Figure 2**. When the ribbon is produced at a higher wheel velocity in melt spinning, the degree of undercooling becomes high because of its thinner thickness and the amount of crystalline layer decreases with wheel velocity. Variations in grain size are often accompanied by changes in dislocation structure and precipitation, which also greatly affect the transformation temperatures. Therefore, it seems to be difficult to investigate the effect of grain size on the transformation temperatures in Ti-Ni alloys. Grain refinement has been reported in literature to decrease the transformation temperatures [6].

The transformation temperature decreased when the velocity of wheel was changed from 30 to 50 m/s, as shown the **Table 1**.
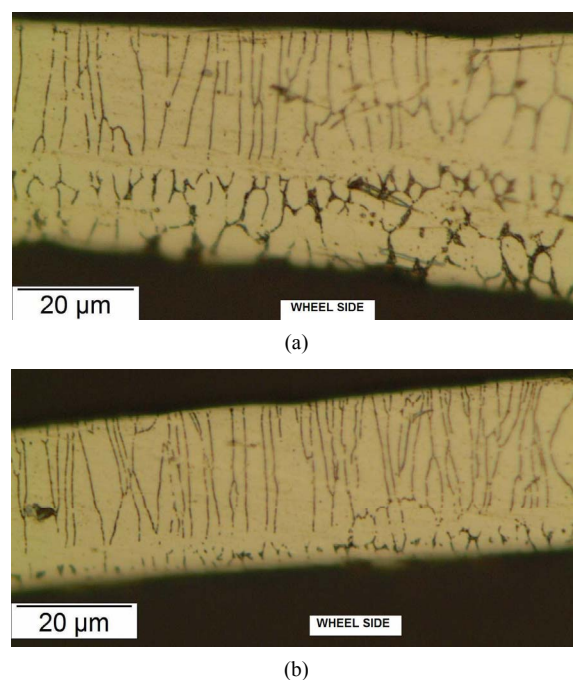

(a)

(b)

Figure 2. Optical micrographs of the ribbons (light brown) fabricated at the wheel velocities of (a) 30 m/s and (b) 50 m/s.

Figure 1. Relationship between ribbon thickness and wheel velocity.

Table 1. Transformation temperatures as cast and cooled in melting spinning.

Cooling Conditions	M$_S$ (°C)	M$_F$ (°C)	A$_S$ (°C)	A$_F$ (°C)	Thickness (μm)
As casting	49.7	34.9	58.0	77.9	-
30 m/s	42.1	29.0	52.0	73.2	41
50 m/s	28.7	22.5	44.2	53.3	30

Figure 3 shows the DSC curve of as-spun grain-size mixed Ti$_{45.3}$Ni$_{54.7}$ ribbons. As can be seen, to ribbons that were fabricated with wheel velocities of 30 m/s the transformation peaks are short with large transformation enthalpies and for the ribbons that were fabricated with wheel velocities of 50 m/s the transformation peaks are broad with short transformation enthalpies. This is because as-spun Ti$_{45}$Ni$_{55}$ ribbons fabricated with wheel velocities of 50 m/s contain greater amount of defects and residual stress. At the same time, the grain size inherent in ribbons is finer than the ribbons that were fabricated with wheel velocities of 30 m/s, as shown in **Figure 2**. The grain boundaries and defects can act as barriers to the martensitic transformation as a result of the extra energy required during transformation [7]. Thus fine-grain ribbons which have lots of grain boundaries would be expected to have lower transformation temperatures and smaller transformation enthalpies, as shown in **Figure 3** and **Table 1**.

NiTi shape memory alloys (SMA) transform martensitically from B2 cubic austenite into monoclinic B19' martensite either directly or via rhombohedral R-phase martensite. The B19' martensite can be obtained either by a single step transformation of B2 → B19', or by a two-step transformation of B2 → R-phase → B19' [8]. Note in **Figure 3** that when ribbons are fabricated with wheel velocities of 30 m/s there are one B2 ⇨ B19' martensitic transformation peak in cooling and heating, but when ribbons were fabricated with wheel velocities of 50 m/s there are B2 ⇨ R and R ⇨ B19' martensitic transformation peaks in cooling and heating and B19' ⇨ R and R ⇨ B2. The occurrence of the multiple martensitic transformations in ribbons of Ti51Ni49 SMA is due to the coexistence of large and small grains distributed in the ribbons. The reason why both R → B19' and B19' → B2 transformations are separated into two peaks which correspond to large and small grains, while the B2 ↔ R transformation is not separated into two peaks is that the B2 ↔ R transformation exhibits much smaller transformation strain than R → B19' and B19' → B2 transformations [6]. **Figure 2** shows a fully crystallized and most of the columnar and small grains are located at the free surface and copper roller surface of the ribbons, respectively. Then, the multi-stage martensitic transformation induced by the inhomogeneous grain size distri-
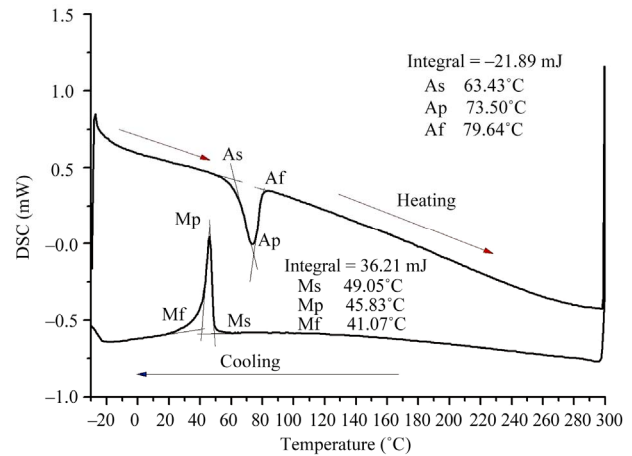
(a)
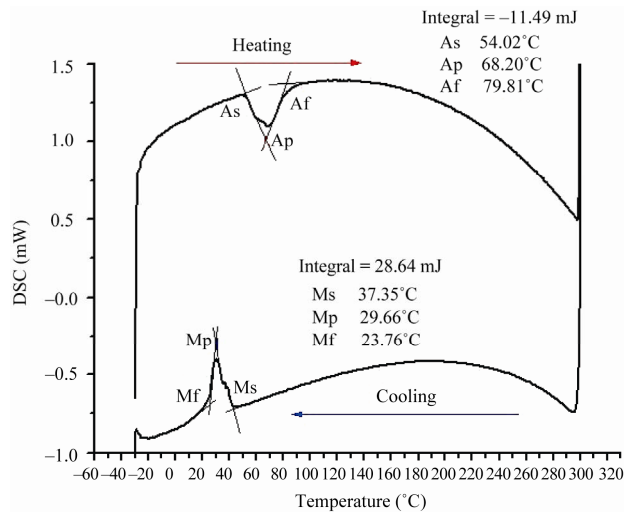
(b)

Figure 3. DSC curves of the ribbons fabricated at the wheel velocities: (a) 30 m/s and (b) 50 m/s.

bution in the ribbon is observed in this study [1]. According to the reported studies, the R-phase appearing in the martensitic transformation of Ti-rich TiNi thin films is induced either by the coherent stress field around the plate-like Guinier-Preston (GP) zones or by the semicoherent stress field around the spherical Ti$_2$Ni precipitates [9-12]. Increasing wheel velocities caused the formation of the R-phase. The as-spun Ti$_{45}$Ni$_{55}$ ribbon has many GP zones, since rapid solidification produces an increase in the number of defects [13] inducing the formation of R-phase.

4. Conclusions

Transformation behavior of melt spun Ti$_{45.3}$Ni$_{54.7}$ alloy ribbons fabricated at different cooling rates by melt spinning was investigated. The increase of the wheel velocity from 30 to 50 m/s results in a decrease of the ribbon

     MSA

thickness. When the ribbon is produced at a higher wheel velocity in melt spinning, the degree of undercooling becomes high because of its thinner thickness. The grain boundaries and defects can act as barriers to the martensitic transformation as a result of the extra energy required during transformation. Thus fine-grain ribbons which have lots of grain boundaries would be expected to have lower transformation temperatures. The DSC result showed that when wheel velocity increases from 30 m/s to 50 m/s the R-phase appears because the as-spun Ti$_{45.3}$Ni$_{54.7}$ ribbon has many Guinier-Preston (GP) zones, induced by the large number of defects. According to the partial-cycled DSC test, we conclude that the peaks of transformations are associated with B2 → R transformation, R → B19' transformation for large grains, R → B19' transformation for small grains during cooling, and B19' → B2 transformation for large grains and B19' → B2 transformation for small grains during heating. The occurrence of the multiple martensitic transformations in ribbons of Ti$_{45}$Ni$_{55}$ SMA is due to the coexistence of large and small grains distributed in the ribbons. The reason why both R → B19' and B19' → B2 transformations are separated into two peaks which correspond to large and small grains, while the B2 ↔ R transformation is not separated into two peaks is that the B2 → R transformation exhibits much smaller transformation strain than R → B19' and B19' → B2 transformations.

5. Acknowledgements

REFERENCES

[1]　Y. Freed and J. Aboudi, "Micromechanical Prediction of the Two-Way Shape Memory Effect in Shape Memory Alloy Composites," *International Journal of Solids and Structures*, Vol. 46, No. 7-8, January 2009, pp. 1634-1647. doi:10.1016/j.ijsolstr.2008.12.004

[2]　Y. Bellouard, "Shape Memory Alloys for Microsystems: A Review from a Material Research Perspective," *Materials Science and Engineering*, Vol. A481-482, February 2008, pp. 582-589.

[3]　H. Morawiec, J. Lelatko, D. Stróz and M. Gigla, "Structure and Properties of Melt-Spun Cu-Al-Ni Shape Memory Alloys," *Materials Science and Engineering*, Vol. A273-275, December 1999, pp. 708-712.

[4]　T. Goryczka and P. Ochin, "Characterization of a Ni$_{50}$Ti$_{50}$ Shape Memory Strip Produced by Twin Roll Casting Technique," *Journal of Materials Processing Technology*, Vol. 162-163, June 2005, pp. 178-183. doi:10.1016/j.jmatprotec.2005.02.029

[5]　"ASTM Standards: Standards Test Method for Determining Average Grain Size," Annual Book of ASTM Standards, 03.01, 2003, p. 256.

[6]　K. N. Lin and S. K. Wu, "Martensitic Transformation of Grain-Size Mixed Ti$_{51}$Ni$_{49}$ Melt-Spun Ribbons," *Journal of Alloys and Compounds*, Vol. 424, No. 1-2, February 2006, pp. 171-175. doi:10.1016/j.jallcom.2006.01.007

[7]　L. Zhang, C. Xie and J. Wu, "Grain Size Estimations of Annealed Ti-Ni Shape Memory Thin Films," *Journal of Alloys and Compounds*, Vol. 432, January 2007, pp. 318-322. doi:10.1016/j.jallcom.2006.06.018

[8]　X. Zhang and H. Sehitoglu, "Crystallography of the B2→R→B19_ Phase Transformations in NiTi," *Materials Science and Engineering*, Vol. A 374, No. 1-2, February 2004, pp. 292-302.

[9]　P. Sittner, M. Landa, P. Lukás and V. Novák, "R-Phase Transformation Phenomena in Thermomechanically Loaded NiTi Polycrystals," *Mechanics of Materials*, Vol. 38, July 2000, pp. 475-492.

[10]　Y. Zhou, J. Zhang, G. Fan, X. Ding, J. Sun, X. Ren and K. Otsuka, "Origin of 2-Stage R-Phase Transformation in Low-Temperature Aged Ni-rich Ti-Ni Alloys," *Acta Materialia*, Vol. 53, January 2005, pp. 5365-5377. doi:10.1016/j.actamat.2005.08.013

[11]　R. Zarnetta, D. Kõnig, C. Zamponi, A. Aghajani, J. Frenzel, G. Eggeler and A. Ludwig, "R-Phase Formation in Ti$_{39}$Ni$_{45}$Cu$_{16}$ Shape Memory Thin Films and Bulk Alloys Discovered by Combinatorial Methods," *Acta Materialia*, Vol. 57, December 2009, pp. 4169-4177. doi:10.1016/j.actamat.2009.05.014

[12]　W. Cai, Y. Murakami and K. Otsuka, "Study of R-Phase Transformation in a Ti-50.7at%Ni Alloy by *In-Situ* Transmission Electron Microscopy Observations," *Materials Science and Engineering*, Vol. A273-275, January 1999, pp. 186-189.

[13]　L. Wu, S. Chang and S. Wu, "Precipitate-Induced R-Phase in Martensitic Transformation of As-spun and Annealed Ti$_{51}$Ni$_{49}$ Ribbons," *Journal of Alloys and Compounds*, Vol. 505, No. 1, June 2010, pp. 76-80. doi:10.1016/j.jallcom.2010.06.019